# The impact of debris flows on structures: practice revisited in light of new scientific results

**Dominique Laigle**[1]; Mathieu Labbé, PhD[2]

## ABSTRACT

Our study aims at determining values of the pressure in the vicinity of a structure subjected to a debris flow impact, and their evolution in time and space, for a given incident flow. We used a numerical model based upon the SPH (smoothed particles hydrodynamics) numerical method and simulated the flow features upstream of an obstacle impacted by a viscoplastic fluid wave. We focus interest on the pressures developed on the structure during the impact. The results are analyzed in view of the incident flow features, characterized by its Froude number Fr. We evidence a transition between what we name the dead-zone impact regime and the jet impact regime. We establish that this transition occurs for values of the Froude number between Fr ≈ 1.3 and 1.5. We evidence the respective roles of the gravitational and kinetic components of the pressure. Finally, we study the spatial distribution of the pressure applied to the obstacle and its evolution with time depending on the impact regime.

## KEYWORDS

debris-flow; SPH; Protection structures; impact pressure

## INTRODUCTION

The understanding and quantification of mudflow and debris flow – structure interactions in terms of modification of the incident flow and impact force applied to the obstacle are of paramount importance for the conception and design of structural countermeasures. In this context, the present study aims at determining local values of the flow velocity and pressure in the vicinity of a structure subjected to a debris-flow impact, as well as the changes in these variables over time and space, for a given incident flow. We use a 2D vertical numerical model based upon the SPH (smoothed particles hydrodynamics) numerical method. SPH is a particular method of treatment of fluid mechanics equations which is suitable for computing highly transitory free surface flows of complex fluids (viscoplastic, granular, etc.) in complex geometries. Thus, it is suitable for the treatment of debris-flow waves – structure interactions. We present our numerical experiments setup aiming at simulating a viscoplastic fluid wave impacting a simple obstacle. We notably focus interest on the pressures developed on the structure during the impact, on their evolution with the incident flow features, and on their spatial distribution over the obstacle. We also analyze our results in terms of physical phenomena explaining the observed pressures.

1 Irstea, Grenoble, FRANCE, Dominique, dominique.laigle@irstea.fr

2 Irstea, UR ETGR Snow avalanche and torrent control, Grenoble center, F-38402 St-Martin-d'Hères, France Univ. F-38041 Grenoble, France

## METHOD

### The SPH method

The SPH (smoothed particle hydrodynamics) method is a mesh-free numerical method initially introduced by Gingold and Monaghan [1977]. It has since found many applications in fluid dynamics. Because of its mesh-free nature, it can handle large deformations of the simulated fluid. It also handles free surfaces naturally. This makes this method particularly well-suited for the simulation of the propagation of mudflows [Rodriguez-Paz and Bonet, 2004], granular materials [Chambon et al., 2011] and their impact on a wall [Laigle et al., 2007; Huang et al., 2011b].

### Virtual experiments layout

Our simulation domain (Figure 1) is derived from the experiments described in Tiberghien et al. [2007]. The experimental setup was designed to generate unsteady flows constituted of a steep front followed by a steady flow of constant depth h. It consisted of a 4 m long 30 cm wide flume with an inclination angle ranging from 0° to 10°. A tank was located upstream of the flume and stored the viscoplastic sample material. This tank was closed by a gate which could be instantaneously removed to release the fluid. A rectangular obstacle of height H was located downstream of the flume. The height H was adjusted from one experiment to another so as to maintain a constant aspect ratio h/H = 0.86. This value was arbitrarily chosen but is the order of magnitude of the ratio encountered in the field when considering real debris flows and protection structures. Simulations were carried out using an improved version of the SPH code presented in Laigle et al. [2007]. The fluid was modelled using about 60000 to 80000 particles, resulting in about 20 particles along the vertical axis in the sheared region of the fluid. Each simulation was run on four cores on dual Xeon computers. The computation time for a single simulation ranged from one to two weeks depending on the number of SPH particles.

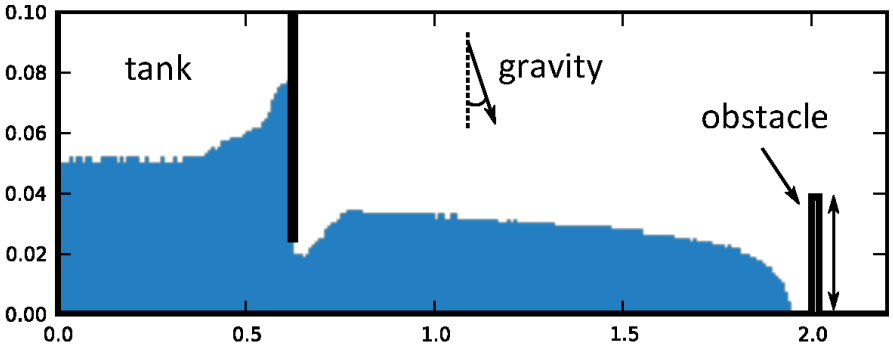


Figure 1: Snapshot of a simulation showing the main features and dimensions of the virtual experiment.

Our objective is to study the evolution of the local flow features in the vicinity of the obstacle for several values of the inclination angle. All other parameters of the virtual experiments (rheological parameters, height of the gate, and fluid level in the tank) are kept constant. This way, each inclination angle is related to a unique incident flow. In order to get a comparative criterion between numerical experiments and field flows, the following results will be presented not only on the basis of the inclination angle. We'll indicate also the value of the Froude number of the incident flow. We adopt here the non-classical definition proposed by Tiberghien et al. [2007] in the framework of their experiments:

$$Fr = \frac{\overline{u}_{front}}{\sqrt{gh\cos\theta}}$$

Formula 1: definition of the Froude number adopted in the framework of the present study

where ufront is not the fluid velocity but an average velocity of the front between the gate and the obstacle. h is the depth of the steady flow following the front propagation and $\theta$ is the inclination angle. The studied inclination angles in the simulations range from 3° to 16°, which corresponds to Froude number values ranging from 0.52 to 2.88, thus of the same order of magnitude as field debris flows.

**Virtual pressure sensors**

One of the goals of this work is to compute the pressure of the fluid in the vicinity of an obstacle. To this effect, we use virtual sensors [Laigle et al., 2007]. These sensors (Figure 2) are constituted of rectangular areas of the simulation domain over which various properties of the fluid are recorded. These properties include the average pressure, velocity, density and depth of the fluid. This is the method we use to compute the pressure on the wall, either at a given location (in which case the height of the sensor is equal to 1 cm, according to the flume experiments by Tiberghien et al. [2007]), or on the whole obstacle (the vertical extent of the sensor matches the height of the wall).

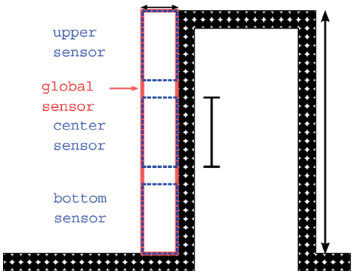


Figure 2: location of the virtual pressure sensors off the upstream face of the obstacle

## RESULTS

### Preliminary results

After Labbé [2015], the observation of general flow features during the impact shows that for gentler slopes, between 3° and 7°, the fluid level goes up gradually along the upstream wall of the obstacle and finally overflows with permanent contact with the upper face of the obstacle. A surface wave looking like a hydraulic bore propagates upstream and a roughly triangular zone of fluid at rest, we name the dead-zone, forms upstream of the obstacle. These observations are coherent with previous experimental results obtained by Tiberghien et al. [2007] among others. For steeper slopes, above 8°, a vertical jet forms immediately when the fluid impacts the obstacle. A dead-zone forms upstream of the obstacle but it is much smaller than at gentle slopes. After the first impact a jet is still present over the obstacle and its angle with the horizontal direction diminishes with time and stabilizes when the steady regime is reached. The jet presents no contact with the upper face of the obstacle. This kind of impact will be referred to as the jet impact regime. At intermediate inclination angles, between 7° and 8°, we observe a transition. While at gentler slopes the size of the dead-zone gets bigger when the inclination reduces, its size is almost constant at steeper slopes.

### Time evolution of the pressure on the obstacle

In this section, we aim at examining the pressure applied by the fluid to the upstream wall of the obstacle. The height of the sensor is identical to the obstacle height. Figure 3 shows the evolution of the pressure versus time for a series of simulations carried out with an increasing flume inclination. We note that a pressure peak is systematically present when the fluid impacts the obstacle as well as a pressure plateau when the steady regime is established. The respective values of these pressures strongly evolve with the flume inclination. On gentle slopes, in the dead-zone regime, a small peak with duration about 0.01 s is observed at the impact followed by a slow increase of the pressure lasting a few seconds. Between 3° and 6°, the first pressure peak, whose intensity is lower than the pressure of the plateau, grows up with increasing inclination. In parallel, the pressure of the plateau diminishes with increasing inclination. From 7° onwards, the peak intensity overcomes the pressure of the plateau. The local minimum in the curve connecting the peak to the plateau disappears at 8°. The duration of the peak increases with slope to reach values about 0.1 s.

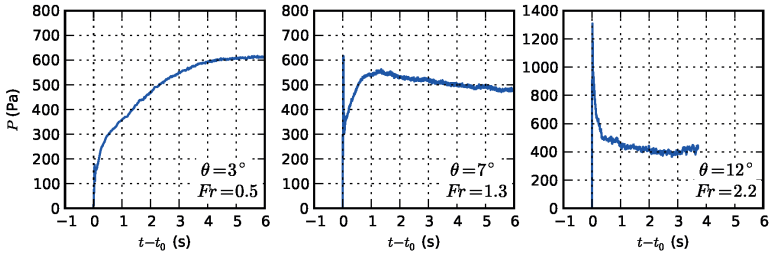


Figure 3: Evolution of the simulated pressure applied to the upstream wall of the obstacle versus time for several values of the virtual flume inclination angle

These results, combined with those of previous section, evidence two different impact regimes (dead-zone regime / jet regime). For the first one the maximum pressure is reached during the plateau when the steady regime is established. For the second one the maximum pressure is reached at the peak which immediately follows the impact. The transition between these regimes is observed between 6° (Fr = 1.12) and 7° (Fr = 1.31).

**Maximum pressures versus Froude number of the incident flow**

In this section we present the maximum pressures recorded by 4 sensors: 3 sensors 1 cm high located at the bottom, centre and top of the upstream face of the obstacle, and 1 global sensor covering all the obstacle height. These data are analyzed in reference to the Froude number (Figure 4). Between Fr = 0.5 en Fr = 1.2 pressures do not vary much for each sensor taken individually and curves are almost parallel. Higher pressures are observed at the bottom and pressures observed at the centre and global sensors are very similar. Between Fr = 1.2 and Fr = 1.6, the global sensor, bottom sensor, centre sensor and upper sensor respectively show a transition. Beyond a Froude value Fr = 1.6, the pressures increase almost linearly with the Froude number and the curves diverge. The pressure is systematically higher at the bottom and lower at the top of the obstacle. Once again, this evidences a transition in the impact regime with some additional information: the transition slightly depends on the position on the obstacle.

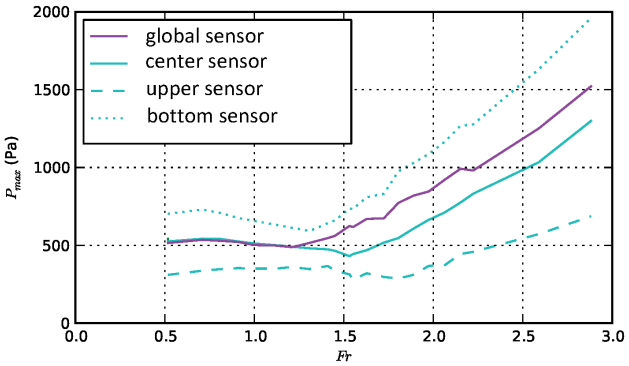


Figure 4: Maximum pressure Pmax recorded by the sensors versus Froude number

**Analysis in terms of gravity and kinetic pressures**

In order to better understand the physics of the impact and to try to deduce rules for a better estimation of impact pressures in the field, we analyse here the respective contributions of the gravity pressure Pg and kinetic pressure Pkin. The kinetic pressure is given by:

$$P_{kin} = \frac{1}{2}\beta\rho\bar{u}^2$$

Formula 2

Where u is the flow velocity, $\rho$ the material density and $\beta$ is a correcting coefficient which value is close to unity. The gravity pressure is given by:

$$P_g = \frac{1}{2}\rho g h \cos\theta$$

Formula 3

These formulas constitute the basis of the models of evaluation of debris-flow impact pressure which can be found in the literature according to a synthesis proposed by Proske et al. (2011). In this section, we consider the maximum mean pressure applied to the whole obstacle Pmax,global (computed using the global sensor) but also the plateau pressure Pplateau (corresponds to the maximum pressure only in the dead-zone regime) and the peak pressure Pp (corresponds to the maximum pressure only in the jet regime).

One can see in Figure 5 that the ratio Pplateau/Pg varies gently and almost linearly with the Froude number. For values of the Froude number higher than 1.2, the Pplateau and the Pmax,global curves diverge and this latter no longer varies linearly with the gravity pressure Pg. For Froude number values lower than 1.2, the ratio Pmax,global/Pg takes values from 2.8 to 3.5.

Figure 6 shows that the ratio Pp/Pkin varies quite quickly with the Froude number when the latter is lower than 1.0 and that the maximum pressure value Pmax,global is higher than the kinetic pressure Pkin. For values of the Froude number higher than 1.2, the Pp and Pmax-,global curves superpose and the ratio Pmax,global /Pkin is almost constant and equals 2. This value is coherent with the theoretical case of a perfect fluid impacting a plate perpendicular to the flow direction. In their synthesis, Proske et al. [2011] note that authors who adopt the kinetic model also propose values of the correcting coefficient from 2.0 for fine slurries to 5.0 for coarse materials.

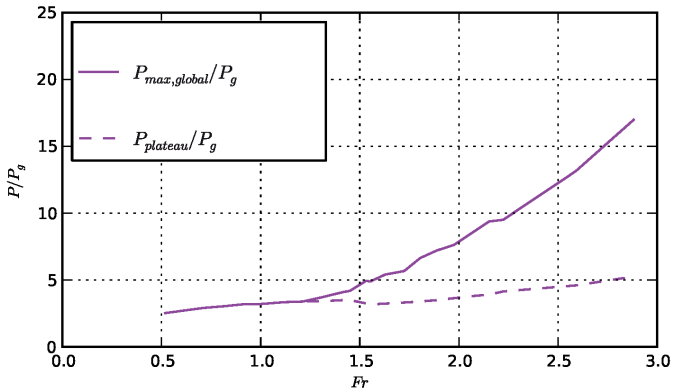


Figure 5: Maximum pressure recorded by the global sensor to gravity pressure ratio Pmax, global/Pg and plateau pressure to gravity pressure ratio Pplateau/Pg versus Froude number

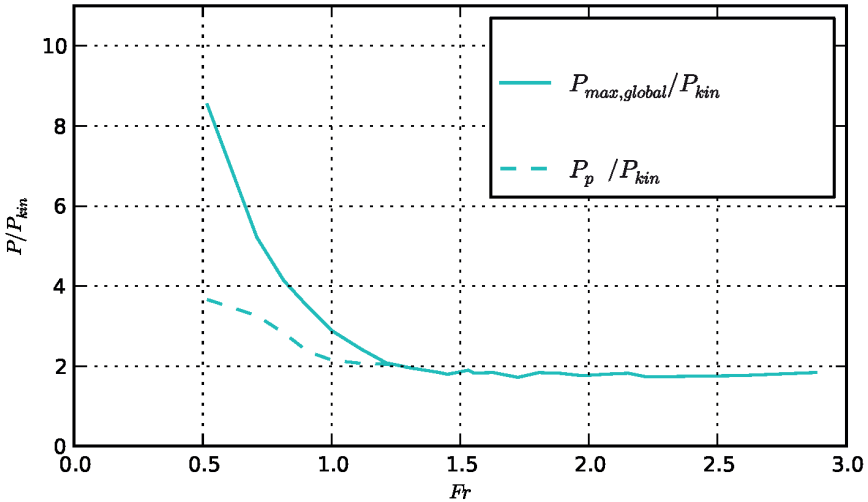


Figure 6: Maximum pressure recorded by the global sensor to kinetic pressure ratio Pmax, global/Pkin and peak pressure to kinetic pressure ratio Pp/Pkin versus Froude number

**Spatial distribution of the pressure**

In this section we investigate the spatial distribution of the pressure applied to the upstream face of the obstacle and its evolution with time considering the impact regime. Whatever the regime, we can observe in Figures 7 and 8 that the first impact takes place at the bottom of the obstacle and the pressure spreads afterwards on the whole obstacle. After a sufficient time, the pressure profile is linear meaning that the plateau is reached and that the gravity pressure is the only contribution at work. One can see in Figure 7 that in the dead-zone regime, the first impact is not very strong and the maximum pressure at any point of the obstacle is clearly observed when the plateau pressure is reached. On the contrary, one can see in Figure 8 that in the jet regime, the first impact is very strong and the maximum pressure, at least at the bottom of the obstacle, is observed during the first impact phase.

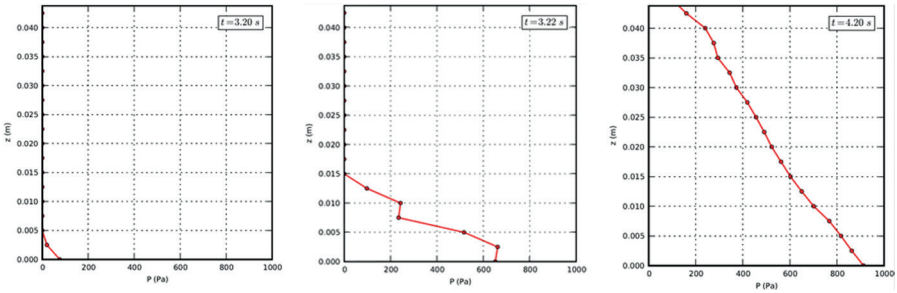


Figure 7: Distribution of the pressure applied to the upstream face of the obstacle at different times of the simulation carried out with Fr = 0.71, $\theta = 4°$ (first time of contact is at 3.187 s)

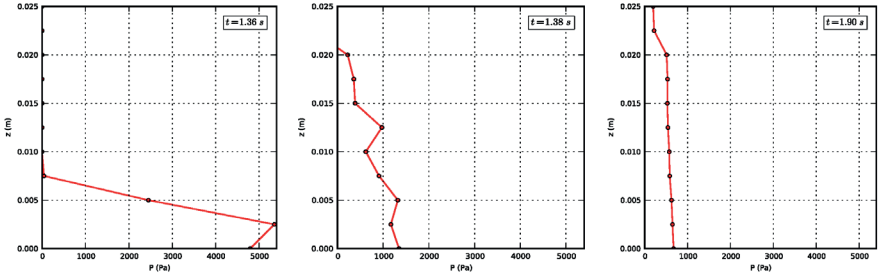


Figure 8: Distribution of the pressure applied to the upstream face of the obstacle at different times of the simulation carried out with Fr = 2.22, $\theta = 12°$ (first time of contact is at 1.354 s)

## CONCLUSIONS

The present study aimed at determining local values of the pressure in the vicinity of a structure subjected to a debris-flow impact, as well as its evolution in time and space, for a given incident flow. To carry out this study, we used a numerical model based upon the SPH numerical method. After briefly presenting SPH, we introduced our numerical experiments setup. In the presence of an obstacle, we simulated the local flows upstream of the obstacle at several times of the impact of a viscoplastic fluid wave. We focused interest on the time evolution and spatial distribution of pressures developed on the structure during the impact. The results were analyzed in view of the features of the incident flow characterized by its Froude number. We evidenced the existence of 2 impact regimes respectively named dead-zone and impact regime with a transition for Froude number values around 1.3 to 1.5. We evidenced the respective contributions of the gravity and kinetic pressures during the impact phase, depending upon the impact regime. We finally analyzed the spatial distribution of the pressure on the obstacle depending on the impact regime.

## REFERENCES

- Chambon, G., Bouvarel, R., Laigle, D. and Naaim, M. (2011): Numerical simulations of granular free-surface flows using smoothed particle hydrodynamics. Journal of Non-Newtonian Fluid Mechanics, 166(12-13): 698-712.
- Gingold, R. and Monaghan, J. (1977): Smoothed particle hydrodynamics-theory and application to non-spherical stars. Monthly Notices of the Royal Astronomical Society, 181: 375-389. ISSN 0035-8711.
- Huang, Y., Dai, Z., Zhang, W. and Chen, Z. (2011): Visual simulation of landslide fluidized movement based on smoothed particle hydrodynamics. Natural Hazards, 59(3): 1225-1238. ISSN 0921-030X.
- Labbé, M. (2015) : Modélisation numérique de l'interaction d'un écoulement de fluide viscoplastique avec un obstacle rigide par la méthode SPH. Application aux laves torrentielles. PhD thesis. Université Grenoble Alpes. (in French)

- Laigle, D., Lachamp, P. and Naaim, M. (2007): SPH-based numerical investigation of mudflow and other complex fluid flow interactions with structures. Computational Geosciences, 11(4): 297-306. ISSN 1420-0597.
- Proske, D., Suda, J., and Hübl, J., (2011): Debris flow impact estimation for breakers. Georisk, 5(2): 143-155.
- Rodriguez-Paz, M. and Bonet, J. (2004): A corrected smooth particle hydrodynamics method for the simulation of debris flows. Numerical Methods for Partial Differential Equations, 20(1): 140-163. ISSN 1098-2426.
- Tiberghien, D., Laigle, D., Naaim, M., Thibert, E. and Ousset, F. (2007): Experimental investigations of interaction between mudflow and an obstacle. In C. Chen and J. J. Major Eds., Proceedings of the International Conference on Debris-Flow Hazards Mitigation: Mechanics, Prediction, and Assessment, Chengdu, China. 281-292.